Heat transfers and energy released in the combustion of fine vegetation fuel beds

V. TIHAY, Y. PEREZ-RAMIREZ, F. MORANDINI, P.A. SANTONI, T. BARBONI

SPE– UMR 6134 CNRS, Université de Corse, Campus Grimaldi, BP 52, 20250 Corte, France

Résumé :

Les transferts thermiques et l'énergie libérée lors de la propagation d'un feu à travers un lit d'aiguilles de pin (Pinus pinaster) ont été étudiés avec et sans pente à l'aide d'un calorimètre à consommation d'oxygène à grande échelle (LSHR). Les résultats ont révélé deux régimes de propagation. Pour les expériences conduites sur une surface plane, la puissance dégagée (HRR) atteint un état quasi-stationnaire tandis que pour les expériences qui se déroulent en pente, la puissance du feu augmente au cours de la propagation. Cette différence est due à une déformation du front de flamme. A plat, le front de feu est en effet linéaire et se propage avec une vitesse presque constante. Au contraire, pour les propagations avec une pente de 20° et un lit de 2m x 1m, le front de feu prend la forme d'un V ce qui entraîne une augmentation de la surface brûlée par unité de temps et donc une augmentation de la puissance du feu lors de la propagation. L'étude a ensuite été consacrée à la caractérisation des transferts thermiques. Dans un premier temps, la fraction convective a été déterminée en utilisant la température enregistrée dans le conduit d'extraction des fumées. Ensuite, les fractions radiatives de la flamme et des braises ont été calculées à partir des mesures de densités de flux radiatifs, de la puissance dégagée et des propriétés géométriques du front de feu. La contribution de chaque type de transfert thermique a ainsi été quantifiée. Les résultats ont montré une augmentation des transferts thermiques par rayonnement lorsque le feu se propage en une pente. Ceci est principalement dû à une augmentation du rayonnement issu des flammes. Toutes ces données donnent des informations globales sur la propagation d'un feu et sont donc très utiles pour améliorer et valider les modèles physiques de propagation de feux de forêt.

Abstract:

The study of the heat transfers and the energy released during the fire spread through beds of pine needles (Pinus pinaster) was conducted under slope and no slope conditions by using a Large Scale Heat Release (LSHR) calorimeter. The results revealed two regimes of propagation. For experiments along a flat surface, the heat release rate (HRR) reached a quasi-steady state whereas for experiments taking place under slope conditions, the HRR increased during the fire spread. This difference was due to a distortion of the fire front. Under no slope conditions, the fire front was indeed linear and propagated with a nearly constant rate of spread. On the contrary, under 20° slope conditions and with a fuel bed of 2 m long and 1 m wide, the fire front had a V-shape leading to an increase of the burnt surface per unit of time and therefore to a rise of the heat release rate during the fire spread. The study was then devoted to the characterization of the heat transfers. Firstly, the convective fraction was determined by using the temperature recorded in the smoke exhaust duct of the LSHR. Then, the radiant fractions of the flame and the embers were calculated from the measurements of radiant heat fluxes, the HRR and the geometrical properties of the fire front. The contribution of each mechanism of heat transfer to the fire spread was therefore quantified. The results showed an increase of the radiation heat transfer, when the fire spread under slope condition, which was mainly due to an increase of the radiation emitted by the flames. All these data give global information on the fire spread and thus they are very useful to improve and validate physical models of wildland fires.

Keywords: Flame spread; Slope; Heat release rate; radiant and convective fractions

1 Introduction

Determining the parameters that control the spread of forest fires is a major objective for the management and the prevention of forest fires. This knowledge is not only crucial for understanding the phenomena but

also for developing and improving models of forest fires. Among all the parameters involved in the fire spread, the role of heat transfer modes still arises many uncertainties. Several studies have reported measurements of radiant or total heat transfers focusing on the heat flux having an impact on the fuel ahead of a fire front [1-3]. Morandini and Silvani [2] showed the existence of two different regimes of fire spread (plume-dominated and wind-driven) that were either dominated by radiation or governed by mixed radiant–convective heat transfer; but they underlined the difficulties for quantifying their proportion. Other studies [4-6] have focused on the percentage of total energy released as radiation and convection. The measurements obtained by Knight and Dando [4] on a bushfire exhibit radiant fraction close to 20 %. Freeborn [5] performed middle infrared measurements. He obtained a radiant fraction of 12.4 % and suggested a convective fraction of about 52%. Kremens [6] used a two-band infrared radiometer to determine the fire radiative energy and found a radiant fraction of 17 %. Tewarson [7] determined the convective fraction by using the Gas Temperature Rise (GTR) calorimetry. For pine wood, a convective fraction of 70.2 % was found, which leads to a radiant fraction equal to 29.8%. In these studies except that of Tewarson [7], the authors assumed a complete combustion and used the heat of combustion instead of the net heat of combustion leading to uncertainties in the estimation of the total heat released. The aim of our study is to understand how the energy is released during fire spread and to quantify the radiant and convective fractions for different conditions (with or without slope). For this, we propose to investigate the effect of the slope on the propagation of a fire across a bed of *Pinus pinaster* needles by using a Large Scale Heat Release Rate Calorimeter (LSHR). We focused mainly on the geometry of the fire front, the heat release rate and the heat transfers.

2 Materials and methods

2.1 Experimental device

Experiments were performed on a 2 m long and 2 m wide inclinable table placed under a 1 MW Large Scale Heat Release (LSHR) calorimeter (Fig. 1). Table inclination was set either to 0° or 20°. At least four experimental replications for each condition of the table were carried out. Fuel beds were made up of pine needles of *Pinus pinaster* covering a surface of 2 m long and 1 m wide, with a loading of 0.9 kg/m². The mean moisture content of pine needles was equal to 7.4 %. The ignition was performed with 4 ml of alcohol over the entire width of the fuel bed edge. The fire experiments were recorded by using two digital cameras: one was located perpendicularly to the fire spread direction (Camera 1) while the other was placed behind the fire front in the direction of propagation (Camera 2). Two radiant heat flux transducers (MEDTHERM 64P-02-24T) were also used to measure heat fluxes during the fire spread (Fig. 1). They were equipped with a Sapphire window (view angle of 150°) and were cooled with circulating water. The first radiant heat flux gauge (RG1) was oriented towards the flame and was placed at the end of the experimental bench, 20 cm above the bed and in the middle of the fire front. The second radiant heat flux gauge (RG2) was located at 1 cm from the end of the experimental bench and halfway up the fuel bed. Finally, a thermocouple (TK) was used to measure the temperature of the combustion gases in the exhaust smoke duct.
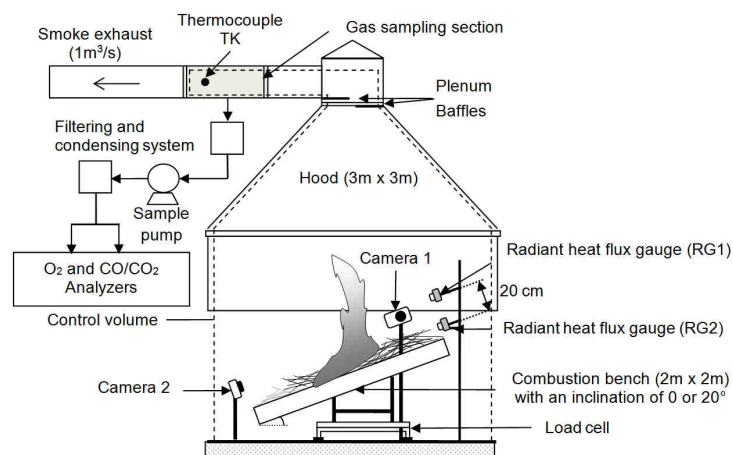

FIG. 1 – Experimental device for the fire spread study

2.2 Methods

The energy released by the combustion of the pine needles was measured by using the LSHR based on the principle of oxygen consumption calorimetry. The exhaust flow velocity and gas volume fractions were measured during the experiments. Then, the heat release rate (HRR) was calculated from these data, according to the formulation derived by Parker [8]. The calculation procedure was detailed in [9]. The characterization of the fire front was carried out from its geometry and position. The time needed to the head of the fire front to cover intervals of 0.25 m along the bench was recorded during the experiments. Flame length (L_f) and the angle between the flame and the vertical axis (β) were determined from photographs taken by camera 1 (Fig. 1). The length of the fire front (L) was obtained from photographs recorded by camera 2 (Fig. 1). When the front was curved (that is to say, for the experiments with a slope), other data were added to complement the information on the fire front. The rear position of the flanks was determined over time by using the pictures taken by the cameras. The angle between the flank and the propagation axis (δ) were obtained from photographs taken by camera 1 (Fig. 1). As the flames on the flanks of the fire front were smaller than in the head and were inclined inwardly of the fire front, we also introduced the length L_h which corresponds to the length of the front, where the flames were the highest. The measurement L_h was performed with camera 2. For each experience, mean values of L, L_h, L_f, β and δ were computed from 30 to 50 images.
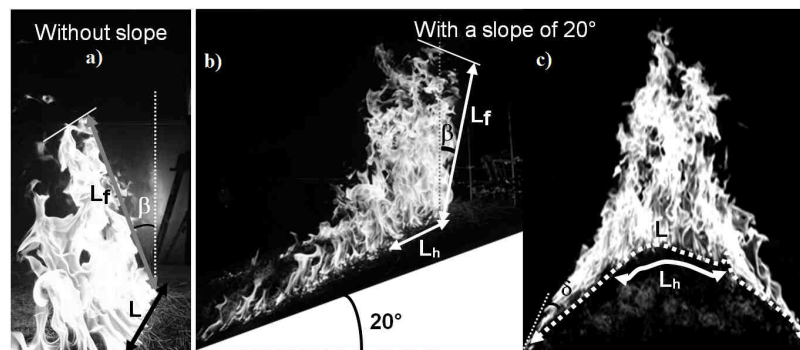

FIG. 2 – Geometric descriptors of the fire front a) no-slope lateral view b) slope lateral view c) slope rear view

3 Results and discussion

3.1 Fire front description

By observing the fire front during propagation experiments, two different behaviors were highlighted. For horizontal fire spread, the fire front exhibited a nearly linear shape (Fig. 2a). The flame length was approximately the same on the entire width of the fuel bed (about 44.4 cm (s.d. 9.3)). The fire front was tilted backward with a mean angle of 14.1° (s.d. 5.0). Conversely, for experiments under a slope of 20°, the flames were inclined forwardly with a mean angle of 5.5° (s.d. 1.0) and fire front had a V-shape with an angle δ equal to 25.1° (s.d. 1.8). According to Dupuy et al. [10], this distortion of the fire front from the initial straight ignition line is explained by the entrainment of air from the sides of the fuel bed area. The mean flame length at the fire front head (located in the middle of the fuel bed) was equal to 70.4 cm (s.d. 7.1). Thus, the flame length increased with increasing slope. However, the flame length exhibit variations along the fire perimeter. Thus, the region of the fire front where the flames was the highest (L_h) corresponds only to a length equal to 27.8 % (s.d. 8.7) of the total length of the fire front (Fig. 2c). On the remaining part of the fire front, the flames were smaller and inclined inwardly of the fire front.

3.2 Heat release rate

For experiments across a flat surface, after 15 s corresponding to ignition phase, the heat release rate became almost constant (about 87 kW (s.d. 21.5)) during about 350 s (Fig. 3a). For our experiments with a

slope of 20°, a quasi-steady state was not observed. The heat release rate continued indeed to increase 120 s until the arrival of the fire front to the end of the table (Fig. 3b). The mean maximum value recorded for the different test fires was 245 kW (s.d. 36.5). The burning time was thus lower for experiments with a slope, because the fire front spread more rapidly (Fig. 3b). Despite these differences, the total heat released did not vary with the slope. The same average value (32.6 MJ (s.d. 1.5)) was indeed obtained regardless propagation conditions. As for the two configurations, the fuel consumption efficiency was equal to 0.97, we obtained the same combustion efficiency. However, for experiments without slope, the heat was released weakly but during a longer time. For our experiments under 20° slope conditions, the heat release rate was much more significant. This difference was due to the fire front shape. Under no slope conditions, the fire front propagated linearly leading to a constant fuel consumption over time and thus to a constant HRR. For our upslope experiments, because of the V-shape of the fire front, the length and depth of the flame front increased during the fire spread. This induced an increase of the surface burnt by the fire per unit of time which in turn produced an increase of the heat release rate.
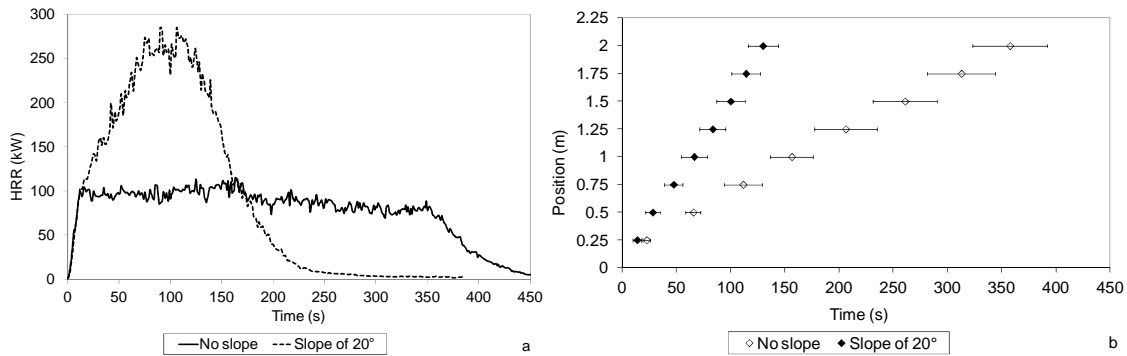

FIG. 3 –a) Heat release rate b) Mean position of the head of the fire front

3.3 Heat transfers

The proportion of convection and radiation in the heat transfers was quantified by using the convective and the radiant fractions. The convective fraction corresponds to the ratio between the convective heat release rate [11] and the heat release rate:

$$\chi_{conv} = \frac{HRR_{conv}}{HRR} = \frac{\dot{M}_{mix} \cdot \int_{T_a}^{T_g} c_{p,mix}(T).dT}{HRR} \tag{1}$$

Where T_a is the ambient temperature, T_g is the gas temperature at duct entry, $c_{p,mix}$ is the specific heat of the mixture at temperature T and $\dot{M}_{mix}$ is the mass flow rate of the chemical compounds-air mixture, determined from the volumetric flow rate of the mixture through the duct. The density and the specific heat of the mixture were taken equal to those of dry air. The gas temperature T_g was calculated from the measurements recorded by the thermocouple TK placed in the gas measuring section (Fig. 1) by considering the heat losses in the duct before the measurement section. According to the propagation conditions, the convective fractions varied significantly. For experiments conducted without slope, the mean convective fraction was equal to 80.2 % (s.d. 4.6), whereas for experiments with a slope, the mean value corresponded to 61.1% (s.d. 2.4) of the heat transfers. The convective fraction was therefore 1.3 times higher for experiments performed along a flat surface than along a slope of 20°.

To determine the fraction of radiation in the heat transfers, the contribution of the flames was distinguished from that of the embers. For the flame, the radiant power was calculated from the heat flux density measurements (q_{RG1}) performed with the radiant heat flux gauge RG1 (Fig. 1) by considering the view factor (F) and the emission surface of the fire front (S_{fl}):

$$\chi_{rad,fl} = \frac{q_{RG1}.S_{fl}}{HRR.F} \tag{2}$$

The determination of the view factor F was based on the Contour Double Integral Formula (CDIF) method, which calculates the view factor between planar polygons. Figure 4 shows a sketch of the configuration adopted for these calculations. For experiments under slope conditions, as the flanks of the fire front consisted of small discontinuous flames, inclined inward the fire front, only the front part where the flames were higher was considered for the calculation of the radiant fraction.

For the embers, the radiant power was calculated from the heat flux density (q_{RG2}) measured with the radiant heat flux gauge RG2. The view factor was assumed to be equal to 1, because the radiant heat flux gauge and the embers were very close (distance equal to 1cm). Embers were modeled by a rectangular parallelepiped having a width of 1 m for experiment without slope. In the case of slope experiments, they were modeled by a trapezoidal prism, with the large base equal to 1 m and the small base of 0.8 m (Fig. 4). Thus:

$$\chi_{rad,em} = \frac{q_{RG2}.S_{em}}{HRR} \tag{3}$$

where HRR is the heat release rate measured when the head of fire front was at the end of the table and S_{em} the embers surface.
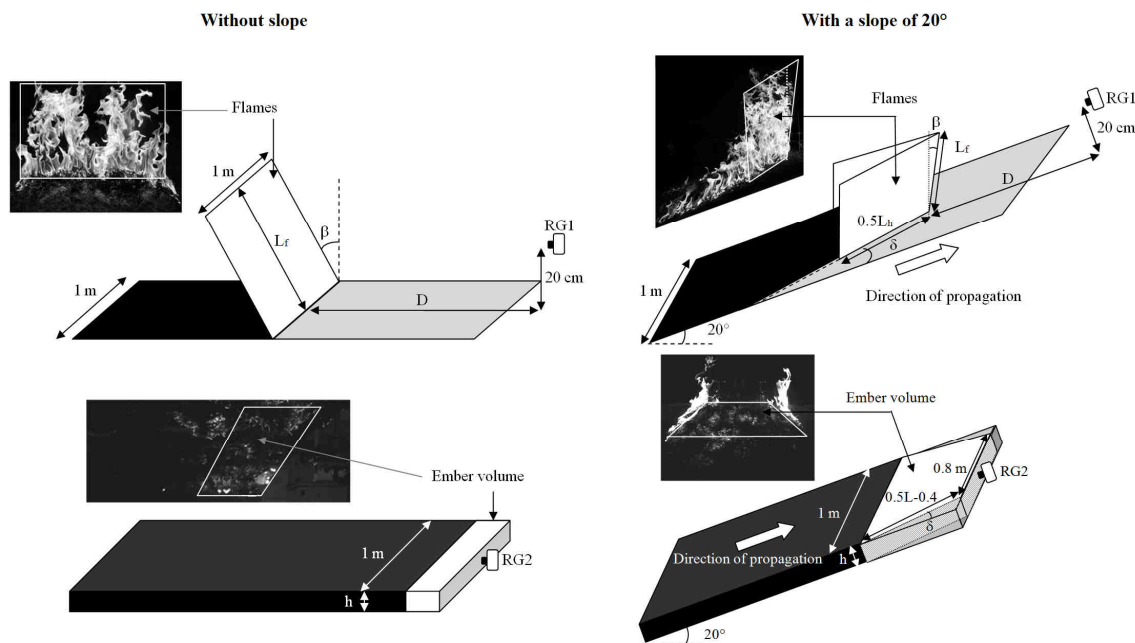

FIG. 4 – Diagrams describing the modeling of the fire front for the calculation of the view factors

For experiments conducted without slope, the mean radiant fractions for the flame and the embers were both equal to 9.9 % (s.d. 0.9 for the flame and 2.0 for the embers). The total radiant fraction corresponds therefore to 19.8%. These results are consistent with literature [4-6]. For experiments with a slope of 20°, the radiant fractions for the flames and the embers were equal to 24.1 % (s.d. 2.6) and 11.8 % (s.d. 2.6), respectively. The overall radiant fraction for upslope fires corresponds to 35.9%. The contribution of the radiation is therefore more significant, when the fire spread occurs under slope conditions. This result is consistent with the decrease observed for the convective fraction. The increase of the radiant fraction of the embers is due to an increase of the volume of embers. For the flames, the radiant fraction was higher because of an increase of the thickness of the flame, which leads to a raise of the emissivity [12]. The sum of the radiant and convective fractions was equal to 100% without slope and to 95.4% with a slope of 20°. We did not obtain 100% with a slope because of an underestimation of the convective fraction. During

the propagation, the suction flow of the hood was not sufficient to evacuate immediately the gases released by the fire and a layer of smoke appeared inside the hood that increased heat losses in the device. This part was not taken into account for the calculation of T_g. For a fire spreading along a flat surface, the ratio of convection to radiation was 4:1 whereas for experiments with a slope of 20°, the part of the radiation increases leading to a ratio of 1.8:1.

Conclusion

In this study, oxygen consumption calorimetry and heat transfer measurements were used to investigate the slope effect on the energy released in the combustion of a bed of pine needles and on the contribution of radiation and convection in fire spread. The main results can be summarized as follows. The total heat released does not vary with the slope. However, this energy is not released in the same way. For experiments without slope, the energy is steadily released during a longer time but reaches a smaller value. For our experiments under 20° slope conditions, the heat release rate increases during the fire spread. These variations are due to the fire front shape. Under no slope conditions, the fire front propagates linearly leading to constant fuel consumption over time. For our experiments under slope conditions, because of the V-shape of the fire front, the length and depth of the flame front increases during the fire spread leading to a raise of the fuel consumption over time. The contribution of convection and radiation to the fire spread varies following the experimental configuration. For experiments across a flat surface, the convective fraction represents about 80% of the heat released by the fire. The remaining part corresponds to the radiation of the flames and of the embers, which participated in an identical manner of the radiation (about 10%). For the experiments with a slope of 20°, the convection represents less than 65% of the heat transfer, released by the fire. The part of the radiation is indeed more significant. The radiation of the flames constitutes about 24%, whereas that of the embers represents about 11% of the heat transfers. Therefore, the common assumption of 30% of radiation must be taken with caution for vegetative fuels. All these results can be helpful for the improvement and validation of physical models of wildland fires.

References

[1] Silvani X., Morandini F., Fire spread experiments in the field: Temperature and heat fluxes measurements, Fire Safety Journal, 44, 279-285, 2009.
[2] Morandini F., Silvani X., Experimental investigation of the physical mechanisms governing the spread of wildfires, International Journal of Wildland Fire, 19, 570-582, 2010.
[3] Dupuy J.L., Maréchal J., Slope effect on laboratory fire spread: contribution of radiation and convection to fuel bed preheating, International Journal of Wildland Fire, 20, 289–307, 2011.
[4] Knight I., Dando M., Radiation above bushfires: Report to State Electricity Commission of Victoria and Electricity Trust of South Australia. National Bushfire Research Unit, CSIRO, Canberra, 1989.
[5] Freeborn P.H., Wooster M.J., Hao W.M., Ryan C.A., Nordgren B.L., Baker S.P., Ichoku C., Relationships between energy release, fuel mass loss and trace gas and aerosol emissions during laboratory biomass fires, Journal of Geophysical Research, 113, D01301, 2008.
[6] Kremens R. L., Dickinson M. B., Bova A. S., Radiant flux density, energy density and fuel consumption in mixed-oak forest surface fires, International Journal of Wildland Fire, 21, 722–730, 2012.
[7] Tewarson A., Generation of Heat and Chemical Compounds in Fires. SFPE Handbook of Fire Protection Engineering, National Fire Protection Association, 2002.
[8] Parker W.J., Calculations of the heat release rate by oxygen consumption for various applications, NBSIR 81–2427–1, 1982.
[9] Santoni P.A., Morandini F., Barboni T., Determination of fireline intensity by oxygen consumption calorimetry, Journal of Thermal Analysis and Calorimetry, 104, 1005-1015, 2011.
[10] Dupuy J.L., Maréchal J., Portier D., Valette J.C., The effects of slope and fuel bed width on laboratory fire behavior, International Journal of Wildland Fire, 20, 272–288, 2011.
[11] Dahlberg M., Error analysis for heat release rate measurement with the SP Industry calorimeter, Swedish Nation Testing and Research Institute, Fire Technology, SP Report 1994:29, 1994.
[12] Boulet P., Parent G., Acem Z., Kaiss A., Billaud Y., Porterie B., Pizzo Y., Picard C., Experimental Investigation of Radiation Emitted by Optically Thin to Optically Thick Wildland Flames, Journal of Combustion, 2011, 37437-1–137437-8, 2011.